

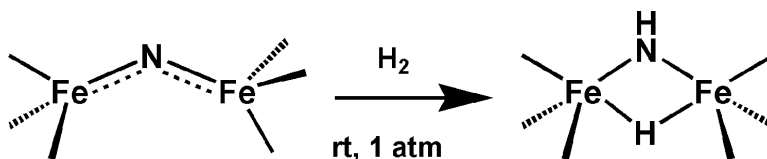
Communication

**Heterolytic H Activation Mediated by Low-Coordinate
 LFe-(η -N)-FeL Complexes to Generate Fe(η -NH)(η -H)Fe Species**

Steven D. Brown, Mark P. Mehn, and Jonas C. Peters

J. Am. Chem. Soc., **2005**, 127 (38), 13146-13147 • DOI: 10.1021/ja0544509 • Publication Date (Web): 03 September 2005

Downloaded from <http://pubs.acs.org> on March 25, 2009



More About This Article

Additional resources and features associated with this article are available within the HTML version:

- Supporting Information
- Links to the 10 articles that cite this article, as of the time of this article download
- Access to high resolution figures
- Links to articles and content related to this article
- Copyright permission to reproduce figures and/or text from this article

[View the Full Text HTML](#)



Heterolytic H₂ Activation Mediated by Low-Coordinate L₃Fe(μ-N)-FeL₃ Complexes to Generate Fe(μ-NH)(μ-H)Fe Species

Steven D. Brown, Mark P. Mehn, and Jonas C. Peters*

Division of Chemistry and Chemical Engineering, Arnold and Mabel Beckman Laboratories of Chemical Synthesis, California Institute of Technology, Pasadena, California 91125

Received July 5, 2005; E-mail: jpeters@caltech.edu

Recently, we described the characterization of an unusual bimetallic bridged iron nitride, $\{([\text{PhBP}_3]\text{Fe})_2(\mu\text{-N})\}^-$, distinct by virtue of the low coordination number (CN = 4) and oxidation state (2+) of its respective iron centers ($[\text{PhBP}_3] = \text{PhB}(\text{CH}_2\text{PPh}_2)_3^-$).^{1,2} Because molecular nitride species might be intermediates of N₂ reduction schemes,³ an avenue of interest was to examine its reactivity toward proton sources¹ and molecular hydrogen.⁴ In the latter context, molecular iron nitrides, whether bridging or terminal, are not known to react with H₂, despite the proposition that such reactions are mechanistically important during the Haber–Bosch ammonia synthesis process.⁵ Herein, we establish the facile heterolysis of H₂ under mild conditions (rt, 1 atm H₂) upon exposure to low-coordinate L₃Fe^{II}(μ-N)-Fe^{II}L₃ and L₃Fe^{III}(μ-N)-Fe^{II}L₃ complexes. The resulting diiron imide–hydride products, L₃Fe(μ-NH)(μ-H)-FeL₃, are structurally unique.^{6,7}

The iron μ-nitrides featured in this study are $\{([\text{PhBP}_3]\text{Fe})_2(\mu\text{-N})\}\{\text{Na}(\text{THF})_5\}$, $\{\mathbf{1}\}\{\text{Na}(\text{THF})_5\}$, a brown complex that consists of two antiferromagnetically coupled high-spin Fe(II) centers,¹ and its neutral one-electron oxidation product, greenish black $\{([\text{PhBP}_3]\text{Fe})_2(\mu\text{-N})\}$ (**2**). Access to the latter species was predicted by the cyclic voltammogram of $\{\mathbf{1}\}^-$, which showed a reversible redox couple at −1.3 V versus Fc^{+/0}. Exposure of $\{\mathbf{1}\}^-$ to numerous oxidants generated varying amounts of the Fe^{III}(μ-N)Fe^{II} species **2**. PCl₃ proved synthetically most reliable in this regard and eliminated NaCl and Cl₂P–PCl₂ as byproducts to afford **2** in 66% crystallized yield. Because the reported structure of $\{\mathbf{1}\}^-$ exhibited an unexpectedly bent Fe–N–Fe linkage and also experienced modest disorder about the N-atom,¹ we undertook the X-ray characterization of single crystals of **2** for comparison. Its core structure is shown in Figure 1 (top).⁸ The Fe–N bond distances of 1.668(2) and 1.683(2) Å for **2** are similar to those observed for $\{\mathbf{1}\}^-$ (Fe–N = 1.675(5) and 1.705(5) Å). The Fe–N–Fe linkage exhibits an even more pronounced bend (142.4(1)°) than that for the case of $\{\mathbf{1}\}^-$. An interesting contrast to the structure of $\{\mathbf{1}\}^-$ is that there is substantial asymmetry about the Fe–P bonds of **2**, perhaps due to a Jahn–Teller distortion that results from placement of one unpaired electron in a nearly degenerate π-orbital set. Specifically, Fe1 exhibits two long and one short Fe–P bond, and Fe2 exhibits two short and one long Fe–P bond. A rhombic signal consistent with the *S* = 1/2 ground state of **2** was observed in its 4 K X-band EPR spectrum.⁹ The low-energy charge transfer and d–d transitions apparent in the optical spectrum of $\{\mathbf{1}\}^-$ appear to be blue-shifted in the spectrum of **2** owing to its higher oxidation state. Also, its solid-state SQUID magnetization data are most consistent with an antiferromagnetically coupled Fe^{II}Fe^{III} spin system. The magnetic moment of **2** increased from 1.82 μ_B at 4 K to 3.40 μ_B at 300 K, most likely indicative of a ground state doublet with thermally accessible higher spin states.

Chemical confirmation of the μ-nitride functionality of **2** was afforded upon its exposure to an atmosphere of CO, which rapidly and quantitatively produced equimolar amounts of the previously

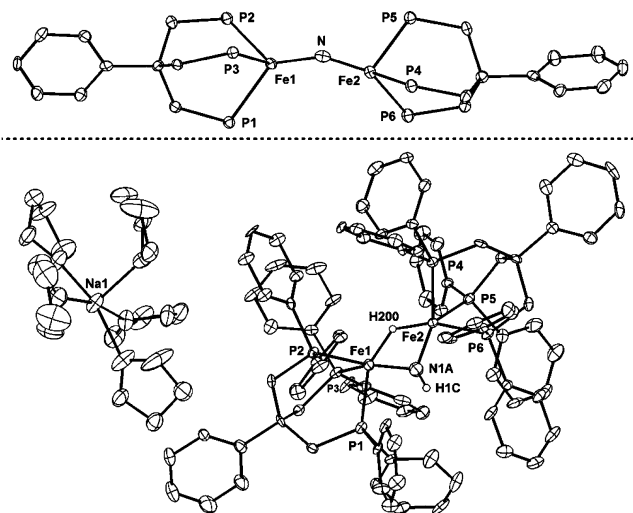
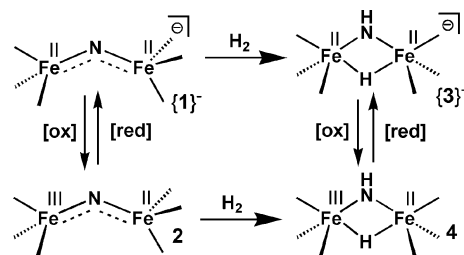
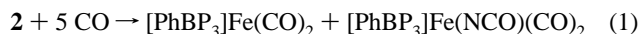


Figure 1. (Top) Solid-state molecular structure of $([\text{PhBP}_3]\text{Fe})_2\mu\text{-N}$ (**2**) with phosphino phenyl groups and two THF solvent molecules removed for clarity. Selected bond lengths (Å) and angles (°): Fe1–N, 1.683(2); Fe2–N, 1.668(2); Fe1–N–Fe2, 142.4(1). (Bottom) Solid-state molecular structure of $[(\text{PhBP}_3)\text{Fe}]_2(\mu\text{-NH})(\mu\text{-H})[\text{Na}(\text{THF})_5]$ (**3**) $\{\text{Na}(\text{THF})_5\}$. Selected bond lengths (Å) and angles (°): Fe1–N1A, 1.826(5); Fe2–N1A, 1.790(5); Fe1–Fe2, 2.6595(9); Fe1–N1A–Fe2, 94.7(3).

Scheme 1



characterized complexes $[\text{PhBP}_3]\text{Fe}(\text{CO})_2$ ¹⁰ and $[\text{PhBP}_3]\text{Fe}(\text{CO})_2\text{(NCO)}$:¹



Exposure of a brown THF solution of $\{\mathbf{1}\}\{\text{Na}(\text{THF})_5\}$ to an atmosphere of H₂ at room temperature resulted in a color change to green within minutes. Isolation and characterization of the resulting product after 2 h demonstrated a net 1,2 H–H addition across the Fe–N–Fe linkage to produce the bridged species $[(\text{PhBP}_3)\text{Fe}]_2(\mu\text{-NH})(\mu\text{-H})[\text{Na}(\text{THF})_5]$ (**3**) $\{\text{Na}(\text{THF})_5\}$ (Scheme 1). The absence of low-energy d–d transitions in the optical spectrum of $\{\mathbf{3}\}^-$ intimated a low-spin diamagnetic system—plausible given the presence of two five-coordinate Fe(II) centers supported by strong-field ligands. Complex $\{\mathbf{3}\}^-$ is indeed diamagnetic and was conveniently characterized by ¹H, ³¹P, and ¹⁵N

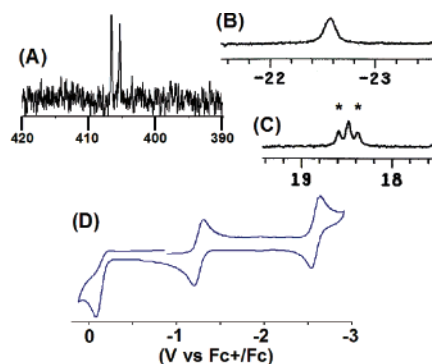


Figure 2. (A) Proton-coupled ^{15}N NMR spectrum, (B) $\mu\text{-H}$ resonance observed in the ^1H NMR spectrum, and (C) $\mu\text{-NH}$ resonance observed in the ^1H NMR spectrum of $\{3\}^-$ (50% ^{15}N). Peaks marked with an asterisk are due to coupling with the ^{15}N nucleus. (D) Cyclic voltammetry of $\{3\}^-$ $\{\text{Na}(\text{THF})_5\}$ in THF (0.3 M [TBA][PF $_6$], 50 mV/s).

NMR spectroscopies. Its ^{31}P NMR spectrum exhibited a singlet resonance at δ 66 ppm, and its ^1H NMR spectrum featured diagnostic resonances at δ +18.5 and -22.4 ppm for the $\mu\text{-NH}$ and $\mu\text{-H}$ ligands, respectively. These resonances were absent in the ^1H NMR spectrum when $\{1\}^-$ was hydrogenated under D_2 . ^{15}N -labeled $\{3\}^-$ (50% ^{15}N) was prepared by the hydrogenation of $\{1\}^-$ (50% ^{15}N) and featured a doublet at δ 406 ppm ($J_{\text{N-H}} = 63$ Hz; Figure 2), shifted significantly upfield from the ^{15}N resonance of its precursor $\{1\}^-$ ($\delta = 801$ ppm (s)).¹ Additionally, the NH resonance at δ +18.5 ppm in the ^1H NMR spectrum of $\{3\}^-$ (50% ^{15}N) exhibited a doublet superimposed on a singlet, resulting from coupling to the 50% ^{15}N label (Figure 2). We were surprised to find that vibrations associated with the imide and hydride ligands could not be observed in the IR spectrum of $\{3\}^-$, regardless of how the samples were prepared (THF/KBr solution, KBr pellet, Nujol).

The cyclic voltammetry of $\{3\}^-$ (Figure 2) demonstrated an irreversible oxidative process at -0.15 V and two low-potential redox events at -1.25 and -2.58 V versus Fc^+/Fc . The reversible event at -1.25 V is indicative of an $\text{Fe}^{\text{III}}\text{Fe}^{\text{II}}/\text{Fe}^{\text{II}}\text{Fe}^{\text{II}}$ redox couple akin to that observed for $\{1\}^-$. This suggests that the hydrogenation of neutral **2** might lead to a stable neutral imide hydride. In fact, exposure of green **2** to an atmosphere of hydrogen generated neutral $\{([\text{PhBP}_3]\text{Fe})_2(\mu\text{-NH})(\mu\text{-H})\}$ (**4**). This product could be alternatively generated by the oxidation of $\{3\}^-$ with $[\text{NO}][\text{PF}_6]$. The lower-potential, pseudo-reversible couple observed in the cyclic voltammogram of $\{3\}^-$ at -2.6 V presumably constitutes an $\text{Fe}^{\text{II}}(\mu\text{-NH})(\mu\text{-H})\text{Fe}^{\text{II}}/\text{Fe}^{\text{II}}(\mu\text{-NH})(\mu\text{-H})\text{Fe}^{\text{I}}$ redox process. Electrochemical access to the reduced $\text{Fe}^{\text{II}}\text{Fe}^{\text{I}}$ species is noteworthy given the recent interest in $\text{Fe}^{\text{II}}\text{Fe}^{\text{I}}$ bimetallic diiron hydride cores as possible intermediates of biological H_2 production.¹¹

The 4 K X-band EPR spectrum of **4** featured the anticipated axial signal for an $S = 1/2$ electronic configuration. The absence of a low-field signal in the spectrum was suggestive of the presence of two low-spin iron centers. Delocalization of its single unpaired electron over both metals was implied by weak phosphorus coupling in the g_{\perp} region arising from all six phosphorus nuclei (simulation provided $A_x = 12$ G). As for its nitride precursor **2**, solid-state SQUID magnetization data for **4** confirmed the presence of one unpaired electron at low temperature ($\mu_{\text{eff}} = 2.12 \mu_{\text{B}}$ at 4 K). We were surprised to find that the moment increased as the temperature was raised to a value of $3.30 \mu_{\text{B}}$ at 300 K, again likely indicating low-lying excited states despite the presumed strong field nature of the system. Distinct from $\{3\}^-$, a readily discernible vibration for the NH ligand (IR; Nujol mull) could be observed at 3319 cm^{-1} for **4**.

Crystals of $\{3\}^-$ suitable for XRD analysis were obtained (Figure 1 (bottom)). The bridging ligands are disordered over two positions as a result of the NH and H ligands alternating positions randomly throughout the crystal. However, electron density attributable to both the imide hydrogen and the hydride ligand could be located in the difference map, and the data were satisfactorily refined when the Fe–H distances were constrained to be equal. The solution was of sufficient quality to unequivocally establish the connectivity of the diiron core and to provide reliable structural data concerning the statistically more prevalent Fe–($\mu\text{-NH}$)–Fe linkage (ca. 70% occupancy). In comparison with nitride $\{1\}^-$, the Fe–N bond lengths for $\{3\}^-$ are expanded by an average distance of 0.118 \AA (Fe–N = $1.790(5)$ and $1.826(5) \text{ \AA}$ for $\{3\}^-$). Also, the Fe–N–Fe bond angle exhibits a severe contraction from $135.9(3)$ to $94.7(3)^\circ$ upon installation of the bridging hydride ligand. The Fe–Fe distance of $2.6588(9) \text{ \AA}$ observed for $\{3\}^-$ is approximately 0.45 \AA shorter than that of $\{1\}^-$ and is similar to the Fe–Fe distances observed in hydrogenase model compounds for which direct iron–iron interactions have been implicated.¹² Our attempts to obtain reliable structural parameters for **4** have been frustrated thus far by severe disorder problems in the crystals we have examined.

In summary, low-valent and low-coordinate bridging iron nitrides stabilized by $[\text{PhBP}_3]$ ligands mediate facile H_2 activation under mild conditions (room temperature, 1 atm H_2). In contrast to previous work from our lab concerning the hydrogenation of low-spin Fe(III) imides,^{4a} complete scission of the Fe–N linkage is not observed. This is presumably due to the presence of an additional metal center that traps the imide–hydride as a bimetallic species.

Acknowledgment. We thank the NIH for financial support (GM-070757 to J.C.P., GM-072291 to M.P.M.), and Dr. Angel J. Di Bilio, Lawrence Henling, and Dr. Michael W. Day for assistance.

Supporting Information Available: Experimental and characterization data; crystallographic data. This material is available free of charge via the Internet at <http://pubs.acs.org>.

References

- (1) Brown, S. B.; Peters, J. C. *J. Am. Chem. Soc.* **2005**, *127*, 1913.
- (2) For some examples of structurally characterized Fe–($\mu\text{-N}$)–Fe linkages, see: (a) Jüstel, T.; Müller, M.; Weyhermüller, T.; Kressl, C.; Bill, E.; Hildebrandt, P.; Lengen, M.; Grodzicki, M.; Trautwein, A. X.; Nuber, B.; Wieghardt, K. *Chem.–Eur. J.* **1999**, *5*, 793. (b) Scheidt, W. R.; Summerville, D. A.; Cohen, I. A. *J. Am. Chem. Soc.* **1976**, *98*, 6623.
- (3) (a) Chatt, J.; Dilworth, J. R.; Richards, R. L. *Chem. Rev.* **1978**, *78*, 589. (b) Buhr, J. D.; Taube, H. *Inorg. Chem.* **1979**, *18*, 2208. (c) Yandulov, D. V.; Schrock, R. R. *Science* **2003**, *301*, 76. (d) Betley, T. A.; Peters, J. C. *J. Am. Chem. Soc.* **2004**, *126*, 6252.
- (4) For examples of H_2 addition to metal–imide-type linkages, see: (a) Brown, S. B.; Peters, J. C. *J. Am. Chem. Soc.* **2004**, *126*, 4539. (b) Cummins, C. C.; Baxter, S. M.; Wolczanski, P. T. *J. Am. Chem. Soc.* **1988**, *110*, 8731. (c) Pool, J. A.; Lobkovsky, E.; Chirik, P. J. *Nature* **2004**, *427*, 527.
- (5) Ertl, G. *Chem. Rec.* **2001**, *1*, 33.
- (6) The $\mu\text{-NH}$ ligand is uncommon. For several structurally related examples, see: (a) Armor, J. N. *Inorg. Chem.* **1978**, *17*, 203. (b) Shaver, M. P.; Fryzuk, M. D. *J. Am. Chem. Soc.* **2005**, *127*, 500. (c) Roesky, H. W.; Bai, Y.; Noltemeyer, M. *Angew. Chem., Int. Ed.* **1989**, *28*, 754.
- (7) ENDOR detection of a paramagnetic iron hydride species formed within the nitrogenase cofactor has been recently reported: Igarashi, R. Y.; Laryukhin, M.; Dos Santos, P. C.; Lee, H. I.; Dean, D. R.; Seefeldt, L. C.; Hoffman, B. M. *J. Am. Chem. Soc.* **2005**, *127*, 6231.
- (8) Complete structural details for **2** and $\{3\}^-$ can be found in the Supporting Information.
- (9) EPR and SQUID magnetization data for **2** and **4**, and optical data for all species, can be found in the Supporting Information.
- (10) Brown, S. B.; Peters, J. C. *J. Am. Chem. Soc.* **2003**, *125*, 322.
- (11) (a) Razavet, M.; Borg, S. J.; George, S. J.; Best, S. P.; Fairhurst, S. A.; Pickett, C. J. *Chem. Commun.* **2002**, 700. (b) Darensbourg, M. Y.; Lyon, E. J.; Zhao, X.; Georgakaki, I. P. *Proc. Natl. Acad. Sci. U.S.A.* **2003**, *100*, 3683.
- (12) (a) Peters, J. W.; Lanzilotta, W. N.; Lemon, B. J.; Seefeldt, L. C. *Science* **1998**, *282*, 1853. (b) Georgakaki, I. P.; Thomson, L. M.; Lyon, E. J.; Hall, M. B.; Darensbourg, M. Y. *Coord. Chem. Rev.* **2003**, *238*, 255. (c) Gloaguen, F.; Lawrence, J. D.; Schmidt, M.; Wilson, S. R.; Rauchfuss, T. B. *J. Am. Chem. Soc.* **2001**, *123*, 12518.

JA0544509